Chiang Mai J. Sci. 2018; 45(6) : 2471-2480
http://epg.science.cmu.ac.th/ejournal/
Contributed Paper

Effect of Acetylene Concentration on Structural Properties of Hydrogenated Amorphous Carbon Films Prepared using Showerhead Plasma Chemical Vapor Deposition

Artit Chingsungnoen* [a], Thananchai Dasri [b], Phitsanu Poolcharuansin [a], Anthika Lakhonchai [a], Nongkhan Tidngim [a], Pitak Eiamchai [c], Noppadon Nuntawong [c] and Vittaya Amornkitbamrung [d]

[a] Technological Plasma Research Unit, Department of Physics, Faculty of Science, Mahasarakham University, Mahasarakham 44150, Thailand.

[b] Faculty of Applied Science and Engineering, Khon Kaen University, Khon Kaen, 40002, Thailand.

[c] Optical Thin-Film Laboratory, Intelligent Devices and Systems Research Unit, National Electronics and Computer Technology Center, Thailand.

[d] Nanotec-KKU Center of Excellence on Advanced Nanomaterials for Energy Production and Storage, Khon Kaen 40002, Thailand.

* Author for correspondence; e-mail: artit.c@msu.ac.th

Received: 5 September 2017
Accepted: 10 November 2017

ABSTRACT

Acetylene/argon plasma was used to deposit hydrogenated amorphous carbon (a-C:H) films using showerhead plasma CVD. The upper electrode was designed like a showerhead to spray gasses onto the grounded electrode and is connected to 10 kHz RF power. The a-C:H films were fabricated with a deposition time of one hour and a substrate temperature of 280 °C for different acetylene concentrations of 3, 4, and 5 %. The result from SEM image shows the thickness of the films increases from 742 nm to 1456 nm. The optical properties of the samples were measured by UV-Vis spectroscopy. It gives the average optical transmittance in the visible light range (400-800 nm) is around 64%, 63%, and 61%. The optical gap energy of the a-C:H films was determined using the Tauc plot method which gives the value around 1.8-2.0 eV. The structural bonding of the prepared films was investigated by x-ray photoelectron spectroscopy and visible Raman spectroscopy with laser wavelengths of 473 nm. All the prepared samples of a-C:H indicated an overall sp^3 content around 18-24%. The Raman spectra were fitted with two Gaussians corresponding to D and G peaks. The peak positions at ~1367 cm^{-1} and ~1594 cm^{-1} were the D and G peaks of the amorphous carbon, which mixes the sp^2 and sp^3 structures.

Keywords: showerhead plasma chemical vapor deposition, hydrogenated amorphous carbon films

1. INTRODUCTION

Hydrogenated amorphous carbon (a-C:H) films are one form of diamond-like carbon (DLC). The a-C:H films or hydrogenated DLC films may contain up to 10-60% hydrogen and are quite different from hydrogen free DLC films. They are amorphous and consist of a mixture of sp^3, which is a diamond matrix, and sp^2 bond graphite clusters embedded in an amorphous sp^3-bonded carbon matrix [1-4]. In a-C:H film with a high hydrogen content (40-60 at. %), most of the sp^3 bonds are hydrogen terminated, and this material is soft, low density, and has a low friction coefficient [5]. These films are usually prepared using the plasma enhanced chemical vapor deposition (PECVD) technique [6]. In a-C:H film with intermediate hydrogen content (20-40 at. %) there are better mechanical properties because there are more c-c sp^3 bonds. They are usually deposited by RF plasma [7] or middle frequency plasma CVD [8]. While hydrogenated tetrahedral amorphous carbon (ta-C:H) films, which have higher sp^3 contents, can be prepared using high-density plasma sources, such as bipolar-type plasma based ion implantation and deposition (bipolar PBII&D) [9-10], filtered cathodic vacuum arc deposition [11], and pulse laser deposition [12]. The properties of a-C:H films can essentially be tailored by controlling the sp^3/sp^2 ratio.

PECVD is one of the most suitable methods for the preparation of a-C:H thin films. Using radio frequency discharge, the precursor gasses are ionized and dissociated, and the radicals as well as ions that impinge onto the substrate, lead to film growth at relatively low temperatures. The a-C:H films initially found applications in improving the tribology of magnetic-head sliders and magnetic storage media [13-14]. For these applications, the contact stresses and operating temperatures are relatively low and, therefore, a-C:H performs well. In recent years, there has been more emphasis on applying a-C:H films to mass-produced mechanical components, particularly in the automotive sector [15]. The films are used to reduce frictional losses under higher stress contact where reliability and coating cost are important to their success [16]. In this work, the a-C:H thin films were deposited using the PECVD technique. To increase the plasma density, the power electrode was designed like a showerhead, which contained small holes with a diameter of one millimeter. The effect of the acetylene concentration in C_2H_2/Ar plasma on the structural properties of a-C:H films was studied.

2. MATERIALS AND METHODS

The plasma reactor was constructed from stainless steel that was cylindrical in shape with a diameter of 26 cm and height of 33 cm. It was equipped with an access door and a view port to observe the process occurring inside the reactor. There were ports for gas supply, vacuum pumping, and electrical feed through for the connection of an RF power supply and heater. The minimum pressure achieved was 1.5 Pa using a two-stage rotary pump. The power electrode (upper) with a diameter of 8.5 cm was designed like a showerhead for spraying the gas mixture into the lower electrode (grounded) with a diameter of 16 cm and a discharge gap length of 5 cm. The power electrode was capacitively coupled to the RF generator working at a fixed frequency of 10 kHz, as shown in Figure 1. The substrate was placed on the grounded electrode.

It is worth noting that, RF discharge at the frequency of 13.56 MHz is typically employed to generate and sustain the plasma in a PECVD system. In addition, the system

also needs an impedance matching circuit to optimize the power delivering to the plasma source. Using a commercial RF power supply with the matching circuit is very effective; however, it requires an excessive cost. In this work, the plasma source was driven by an in-house RF power supply with a rather low frequency of 10 kHz. Using the chosen frequency, a conventional signal amplifier in conjunction with a ferrite core transformer can be employed for the plasma generation. The power reflection between the power supply and the plasma source can be negligible at the given frequency. Therefore, the power supply can directly connect to the plasma source without any impedance matching circuit.

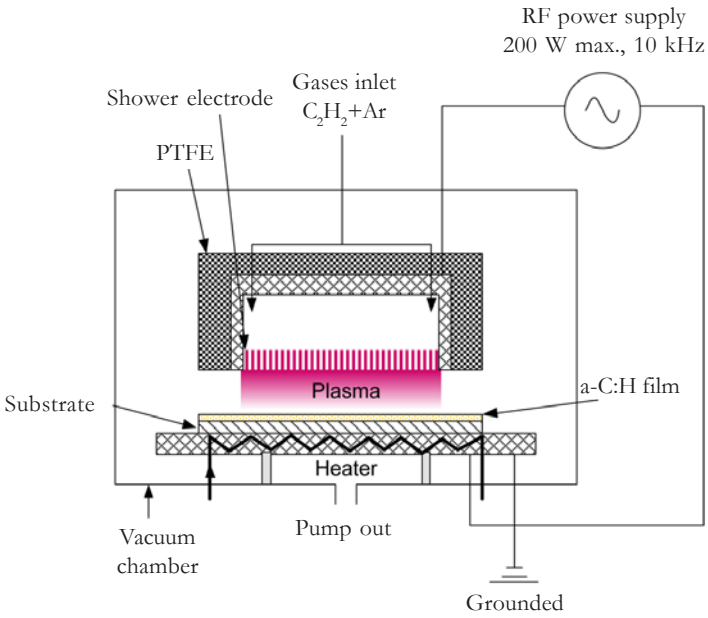

Figure 1. Experimental setup for a-C:H coating (The diagram is not to scale).

The working pressure varied from 47.4 Pa to 52.6 Pa. The glass substrates were pretreated for 25 minutes in an argon plasma at the working pressure of 47.4 Pa and flow rate of 60 sccm (standard cubic centimeters per minute). The acetylene gas used as a hydrocarbon source was supplied into the reactor for the acetylene concentration of 3%, 4%, and 5%. Table 1 shows the deposition conditions used for preparing of a-C:H films. They were deposited using an RF power of 80 W and deposition time of one hour. The substrate temperature during the deposition was kept at 280 °C, while the post plasma treatment for 10 minutes was conducted in situ after the deposition process with argon plasma at the same power and pressure.

The optical transmission was measured using UV-Vis spectrometer (UV-1800, SHIMADZU) at wavelengths 200 and 1100 nm with a resolution of 1 nm. The visible Raman spectra were collected with a 50× objective lens and the laser power was 1 mW. The spectral resolution of the apparatus was 1 cm^{-1}. Typical data acquisition times were in the range of 50 seconds. All the visible Raman spectra were collected by subtracting the background. The spectra were recorded in the range of 100-2000 cm^{-1} to allow the reliable fitting of the D and G peaks.

Table 1. Experimental conditions used to prepare a-C:H films.

Acetylene Concentration (%)	Total flow rate (sccm)	T_s (°C)	Working pressure (Pa)
3	60	280	51.3
4	60	280	50.0
5	60	280	47.4

3. RESULTS AND DISCUSSION

Scanning electron microscopy (SEM) was used to examine film surface and thickness with sub-micron size features. Figure 2 shows SEM micrographs of the a-C:H films grown at different acetylene concentration (a) 3%, (b) 4%, and (c) 5%. Figure 3 shows representative SEM micrographs for cross-sectioned a-C:H-coated on glass. The average film thickness of the a-C:H films, measured over ten different areas, shows approximately 742 ± 18 nm, 1132 ± 144 nm, and 1456 ± 107 nm, respectively. Their deposition rates are calculated by dividing the film thickness over deposition time. They are found to be 2.06 ± 0.05 Å/s, 3.14 ± 0.40 Å/s, and 4.04 ± 0.30 Å/s, respectively. It can be seen that at low deposition rates (2 Å/s) the a-C:H film is rather smooth and exhibits uniformly thickness. Increasing of acetylene concentration will increase the deposition rate. At higher deposition rates, the number of carbon atoms arriving onto the surface per unit time is higher. Figure 2c shows the significant increase in surface roughness of the a-C:H film deposited with 5% of acetylene concentration. It is therefore believed that most of the adsorptions atoms which have insufficient time to migrate to sites to be covered by the coming atom and as a result, the surface of the film is very rough.

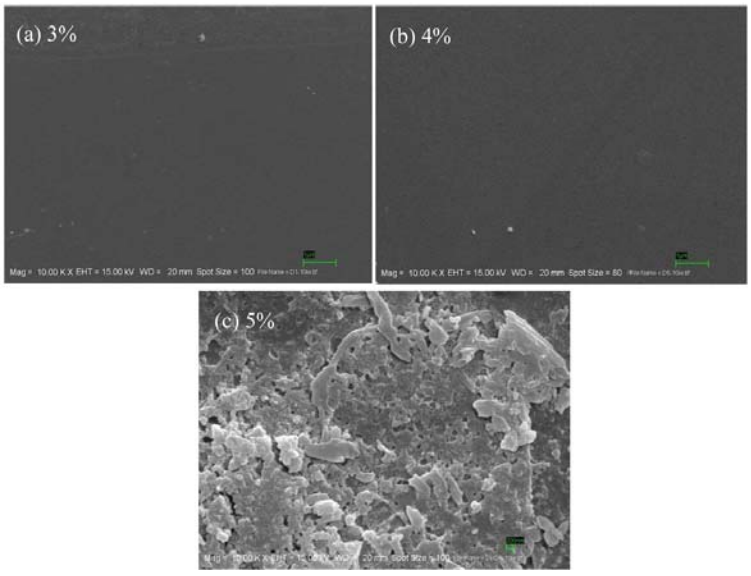

Figure 2. SEM images of a-C:H films produced at different acetylene concentration (a) 3%, (b) 4%, and (c) 5%.

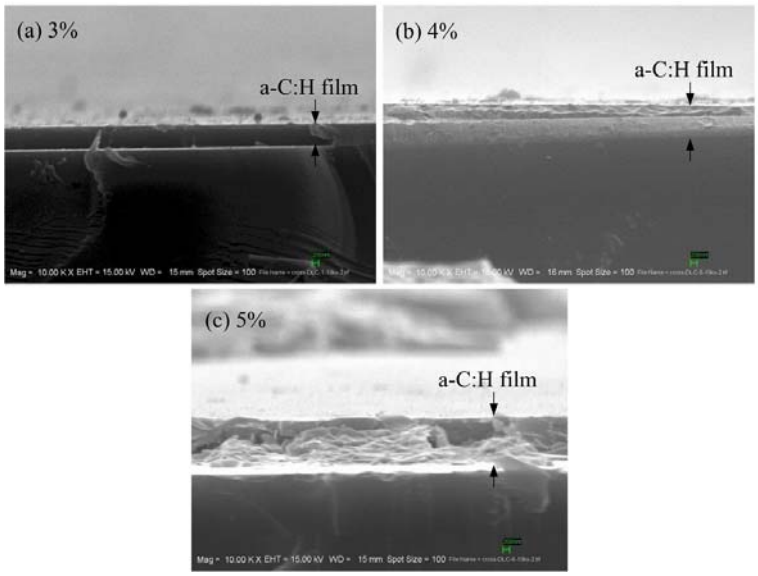

Figure 3. SEM images for cross-sectioned a-C:H-coated on glass produced at different acetylene concentration (a) 3%, (b) 4%, and (c) 5%.

The optical transmission spectra of a-C:H films deposited on the glass substrate was recorded as a function of wavelength in the range of 200 to 1100 nm as shown in Figure 4. It shows that the average optical transmittance of the samples in the visible light range (400-800 nm) is around 64%, 63%, and 61% for the a-C:H films deposited with 3%, 4%, and 5% of acetylene concentration. From the transmission data, the optical band gap energy (E_g) of the a-C:H films can be determined. E_g can be deduced by using the Tauc relationship. The coefficient of absorption α over the threshold of fundamental absorption follows a dependency $(\alpha h\upsilon)^{1/2} = B(E_g - h\upsilon)$, where B is a constant and is the photon energy. Figure 5 shows a typical Tauc plot of a-C:H films deposited with 3% of acetylene concentration. The indirect band gap of a-C:H films was evaluated by extrapolating the straight line part of the curve $(\alpha h\upsilon)^{1/2} = 0$ that gives the optical band gap energy equal to 1.87 eV. Casiraghi et al. [17] summarized that for a-C:H films which the optical band gap energy is between 1-2 eV will have H content around 20-40 at.%. Figure 6 shows the optical band gap energy and transmittance in the visible spectrum of the a-C:H films as a function of film thickness. It is seen that the average optical transmittance slightly decreases with the increasing of film thickness, indicating that the film thickness has little effects on the transparency of the films in the visible light range. Increasing of acetylene concentration used in PECVD has an effect directly to the sp^3 content that achieved mainly by H saturating C=C bonds. Increasing of H content reduces the sp^2 cluster size and increases the optical band gap energy of a-C:H films.

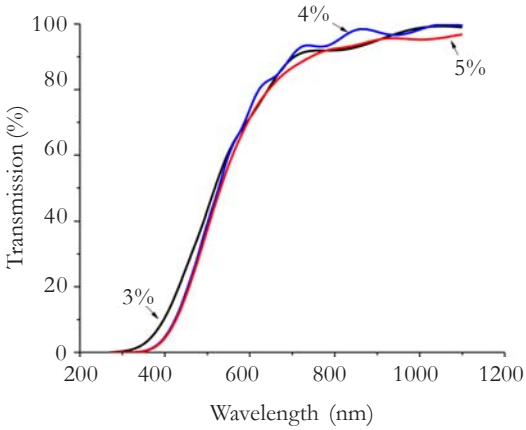

Figure 4. Transmission spectra of a-C:H films deposited by showerhead plasma CVD at different acetylene concentration.

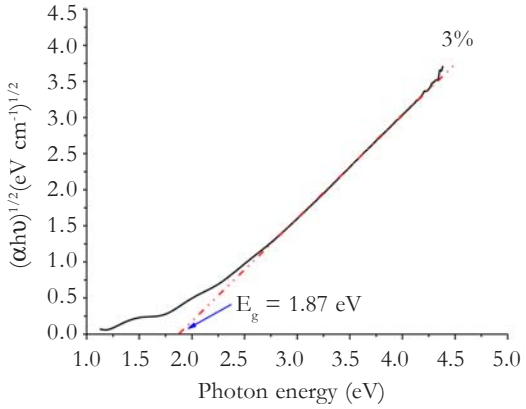

Figure 5. The typical Tauc plot of a-C:H films deposited with 3% of acetylene concentration.

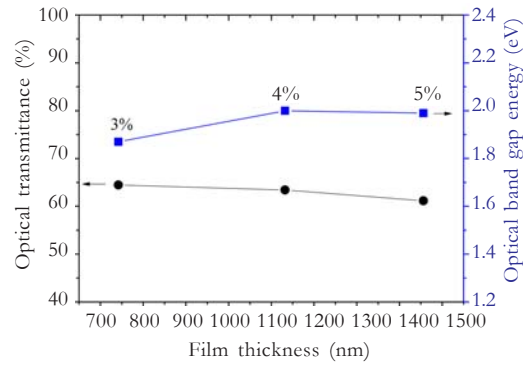

Figure 6. Optical band gap energy and transmittance in the visible spectrum of the a-C:H films as a function of film thickness.

X-ray photoelectron spectroscopy (XPS) was used to distinguish between sp^2 and sp^3 carbon of a-C:H surfaces. The C1s spectrum from a sample with high concentration of sp^2 carbon will have a broad, asymmetric tail towards higher binding energy. While a sample with high concentrations of sp^3-bonded carbon, the C1s peak will have a more symmetric shape and will also be slightly shifted to higher binding energy. Figure 7 represents the broad scan XPS spectra of each sample which as expected that the intense C 1s peak (~285 eV) dominates the spectra. All spectra show N 1s (~400 eV) and O 1s (532.5 eV) contributions. The oxygen atom can be incorporated into the surface of a-C:H films due to air exposure while nitrogen from contamination may have been deposited during the sample preparation. Figure 8 shows the C1s high-resolution spectra of carbon from all the samples. The spectra were decomposed into four components. The first component is found at 285.0 ± 0.1 eV and corresponds to sp^2 carbon atoms, while the second at 286.1 ± 0.1 eV corresponds to sp^3 carbon atoms. The third peak of smaller intensity is found at 287.1 eV ± 0.1 eV which attributed to C-N bonds. The last peak of lowest intensity is found at 288.3 ± 0.2 eV that associated with C-O bonds [18-19]. The sp^3 carbon atom content was then extracted as the ratio of the corresponding peak area over the total C 1s peak area. The calculated results show that sp^3 content is about 23.8%, 18.8%, and 19.6% corresponding to a-C:H films prepared using 3%, 4%, and 5% of acetylene concentration, respectively. However, it should be noted that the sp^3 content calculated using XPS data will represent only the surface values, and may slightly differ from the bulk. All the prepared samples of a-C:H indicated an overall sp^3 content of interval 18-24%, therefore they

have a high sp^2 content and sp^2 clustering and can be classified as graphite-like a-C:H.

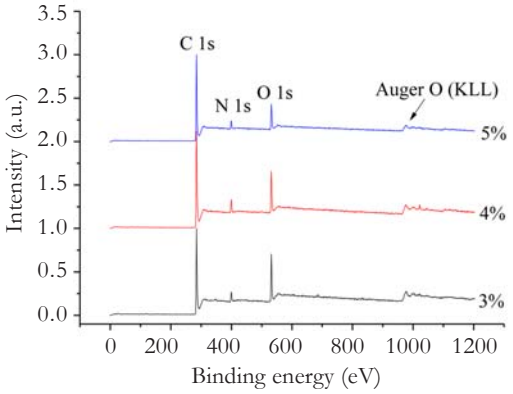

Figure 7. XPS survey spectra from an a-C:H film grown at different acetylene concentration.

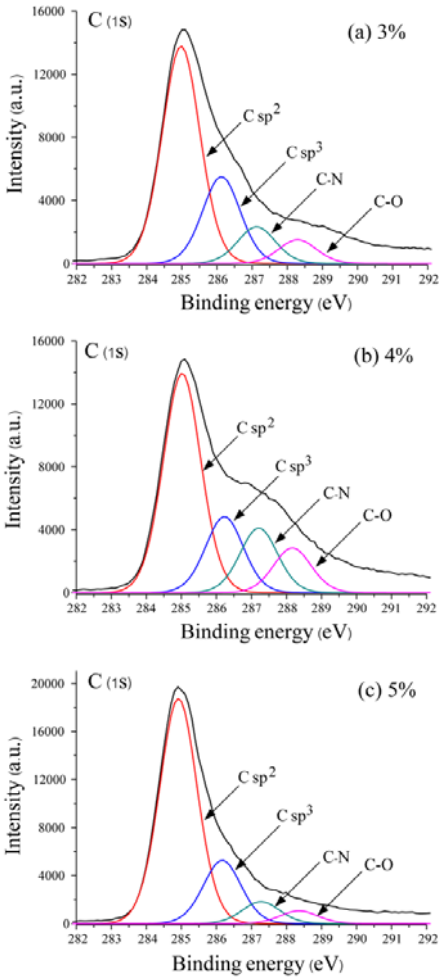

Figure 8. C1s XPS spectra of the a-C:H films deposited at different acetylene concentration.

The structural properties of the a-C:H films were measured using visible Raman spectroscopy. The method is based on an analysis of the spectra, which in general show two features at approximately 1560-1620 cm^{-1} (G peak) and 1360-1420 cm^{-1} (D peak). The G and D peaks are due to sp^2 sites only. The G peak is due to the bond stretching of all pairs of sp^2 atoms in both rings and chains. The D peak is due to the breathing vibration of six-fold aromatic rings, which is activated by disorder [20-24]. The 473 nm HeNe laser was preferred as the excitation source due to its energies corresponding to the $\pi \rightarrow \pi^*$ transition of the sp^2 electronic configuration. The Raman spectra measurements for all the films corresponding to the samples described in Table 1 are shown in Figure 9. The Raman spectra were fitted with two Gaussians corresponding to D and G peaks. The peaks at ~1367 cm^{-1} and ~1594 cm^{-1} are the D and G peaks of the amorphous carbon. The parameters of the two peaks used for the characterization of the a-C:H films are full width at half maximum of the G peak ($FWHM_G$) and D peak ($FWHM_D$), D position (ω_D), G position (ω_G), and the intensity ratio of the D to G peaks (I(D)/I(G)). These parameters are shown in Table 2.

Figure 10 shows the variation in the G position and the sp^3 content as a function of the acetylene concentration in the Ar plasma. It can be seen that the G position decreased rapidly with an increase in the acetylene concentration from 3% to 4%, and after that there was slight variation in the G position around 1593 $cm^{-1} < \omega_G < 1594$ cm^{-1}. The similar effect is found for the sp^3 content. Ferrari and Robertson [20-21] summarized experimental data from different sources and shown that the sp^3 content in the a-C:H films is directly related to the G position in the films. A similar characteristic was shown by Tamor *et al.* [25].

Table 2. Parameters of two peaks used for characterization of a-C:H films.

Acetylene concentration (%)	$FWHM_D$ (cm^{-1})	$FWHM_G$ (cm^{-1})	ω_D (cm^{-1})	ω_G (cm^{-1})	I(D)/I(G)
3%	58.85	68.70	1363.7	1595.7	0.22
4%	83.54	94.89	1371.0	1593.7	0.17
5%	92.88	94.84	1368.2	1593.4	0.22

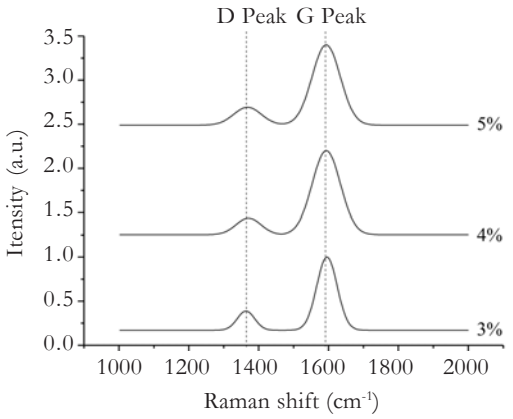

Figure 9. Raman spectra of a-C:H films using a 473 nm HeNe laser as excitation source.

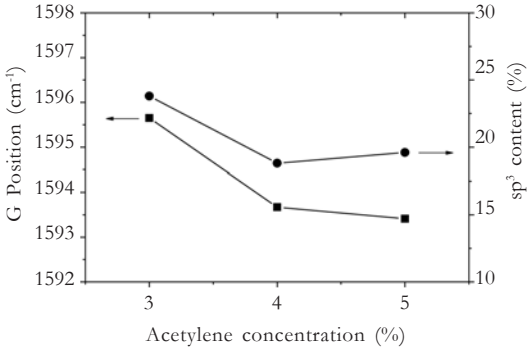

Figure 10. G position and sp^3 content as a function of acetylene concentration.

4. CONCLUSIONS

In this research, a-C:H films were deposited on a glass substrate using the plasma enhanced chemical vapor deposition technique. The power electrode was designed like a showerhead to spray the source gases onto the top surface of the substrate. The film uniformity in the radial direction did not to be studied. However, for low working pressure (≈ 50 Pa) the neutral species distribution is almost constant throughout the reactor. Therefore the effect of deposition rate on the radial distribution can be neglected. The acetylene/argon plasma was generated with an RF input power of 80 W and a frequency of 10 kHz. The a-C:H films were fabricated with a deposition time of one hour and a substrate temperature of 280 °C for different acetylene concentrations of 3, 4, and 5 %. The result from SEM image shows that the thickness of the film increases with the increasing of acetylene concentration. The average optical transmittance of the samples in the visible light range (400-800 nm) is around 64%, 63%, and 61% for the a-C:H films deposited with 3%, 4%, and 5%, respectively. The optical gap energy of the a-C:H films was determined using the Tauc plot method which gives the E_g around 1.8-2.0 eV. X-ray photoelectron spectroscopy was used to distinguish between sp^2 and sp^3 carbon of a-C:H surfaces. All the prepared samples of a-C:H indicated an overall sp^3 content around 18-24%. The laser wavelength of 473 nm was used to the excitation source for Raman spectroscopy. The Raman spectra were fitted with two Gaussians corresponding to D and G peaks. The peak positions at ~1367 cm^{-1} and ~1594 cm^{-1} were the D and G peaks of the amorphous carbon. A small sp^2 cluster size in the a-C:H films

should be correlated with the I(D)/I(G) ratio and $FWHM_G$. This means that the films have a high sp^2 content and sp^2 clustering, so they can be classified as graphite-like a-C:H and should have more C-C sp^3 bonds than the polymer-like a-C:H films due to the shower plasma source being able to generate density plasma together with heating the substrate. The authors prefer to use the lower acetylene concentration (3%) which will give the lower deposition rate and exhibit a-C:H films more uniformly and density. Due to the adsorptions atoms have sufficient time to migrate to sites to be covered by the coming atom. Moreover the a-C:H films (3%) which have lower sp^3/sp^2 ratio tend to appear the lower friction coefficient resulted from the higher H content. Thus, they should have better mechanical properties that correlate to many of the beneficial properties of diamond-like carbon, such as low friction, high hardness, and electrochemical inertness.

ACKNOWLEDGEMENTS

This Research was financially supported by Mahasarakham University Grant Year 2018, the Division of Research Administration, Research, and Technology Transfer Affairs, Khon Kaen University, and the Nanotechnology Center (NANOTEC), NSTDA, Ministry of Science and Technology, Thailand through its Center of Excellence Network program. The authors would like to thank Mr. Harunobu Maeda for assistance with the Raman technique.

REFERENCES

[1] Robertson J., *Mater. Sci. Eng.*, 2002; **R 37**: 129-281. DOI 10.1016/S0927-796X(02)00005-0.

[2] Kurlan F.P., Klein A.N. and Hotza D., *Rev. Adv. Sci.*, 2013; **34**: 165-172.

[3] Zhang S., Fu Y.Q., Bui X.L. and Du H.J., *Int. J. Nanosci.*, 2004; **3**: 797-802. DOI 10.1142/S0219581X04002693.

[4] Kim D.S., *Korean J. Chem. Eng.*, 2005; **22**: 639-642. DOI 10.1007/BF02706657.

[5] Ferrari A.C., *Diam. Relat. Mater.*, 2002; **11**: 1053-1061.

[6] Capote G., Freire F.L., Jacobsohn L.G. and Mariotto G., *Diam. Relat. Mater.*, 2011; **13**: 1454-1458. DOI 10.1016/j.diamond.2003.11.030.

[7] Ha P.C.T., McKenzie D.R., Bilek M.M.M., Kwok S.C.H., Chu P.K. and Tay B.K., *Surf. Coat. Technol.*, 2007; **201**: 6734-6736. DOI 10.1016/j.surfcoat.2006.09.048.

[8] Guo G., Tang G., Wang Y., Ma X., Sun M., Wang L. and Yukimura K., *Appl. Surf. Sci.*, 2011; **257**: 4738-4742. DOI 10.1016/j.apsusc.2010.12.150.

[9] Park W., Tokioka H., Tanaka M. and Choi J., *J. Phys. D: Appl. Phys.*, 2014; **47**: 335306. DOI 10.1088/0022-3727/47/33/335306.

[10] Hirata Y., Kato T. and Choi J., *Int. J. Refract. Met. Hard Mater.*, 2015; **49**: 392-399. DOI 10.1016/j.ijrmhm.2014.08.005.

[11] Lee S., Yoon S.H., Kim J.K. and Kim D.G., *Jpn. J. Appl. Phys.*, 2011; **50**: 01AH01. DOI 10.1143/JJAP.50.01AH01.

[12] Bonelli M., Ferrari A.C., Fioravanti A.P., Miotello A. and Ossi P.M., *Mat. Res. Soc. Symp. Proc.*, 2000; **593**: 359363.

[13] Vetter J., *Surf. Coat. Technol.*, 2014; **257**: 213-240. DOI 10.1016/j.surfcoat.2014.08.017.

[14] Moriguchi H., Ohara H. and Tsujioka M., *Sci. Technol. Rev.*, 2016; **82**: 53-58.

[15] Hainsworth S.V. and Uhure N.J., *Int. Mater. Rev.*, 2006; **52**: 153-174. DOI 10.1179/174328007X160272.

[16] Erdemir A. and Donnet C., *J. Phys. D: Appl. Phys.*, 2006; **39**: R311-R327. DOI 10.1088/0022-3727/39/18/R01.

[17] Casiraghi C., Ferrari A.C. and Robertson J., *Phys. Rev. B*, 2005; **72**: 085401. DOI 10.1103/PhysRevB.72.085401.

[18] Merel P., Tabbal M., Chaker M., Moisa S. and Margot J., *Appl. Surf. Sci.*, 1998; **136**: 105-110. DOI 10.1016/S0169-4332 (98)00319-5.

[19] Cloutier M., Harnagea C., Hale P., Seddiki O., Rosei F. and Mantovani D., *Diam. Relat. Mater.*, 2014; **48**: 65-72. DOI 10.1016/j.diamond.2014.07.002.

[20] Ferrari A.C. and Robertson J., *Philos. Tr. R. Soc. Lond. A*, 2004; **362**: 2477-2512. DOI 10.1098/rsta.2004.1452.

[21] Ferrari A.C. and Robertson J., *Phys. Rev. B*, 2001; **64**: 075414. DOI 10.1103/ PhysRevB.64.075414.

[22] Rose F., Wang N., Smith R., Qi-Fan X., Inaba H., Matsumura T., Saito Y., Matsumoto H., Dai Q., Marchon B., Mangolini F. and Carpick R.W., *J. Appl. Phys.*, 2014; **116**: 123516. DOI 10.1063/ 1.4896838.

[23] Schwan J., Ulrich S., Batori V. and Ehrhardt H., *J. Appl. Phys.*, 1996; **80**: 440-447. DOI 10.1063/1.362745.

[24] Davis C.A., Silva S.R.P., Dunin-Borkowski R.E., Amaratunga G.A.J., Knowles K.M. and Stobbs W.M., *Phys. Rev. Lett.*, 1995; **75**: 4258. DOI 10.1103/ PhysRevLett.75.4258.

[25] Tamor M.A., Vassell W.C. and Carduner K.R., *Appl. Phys. Lett.*, 1991; **58**: 592. DOI 10.1063/1.104597.